# Temperature and immigration effects on quorum sensing in the biofilms of anaerobic membrane bioreactors


## Abstract

Quorum sensing (QS), a microbial communication mechanism modulated by acyl homoserine lactone (AHL) molecules impacts biofilm formation in bioreactors. This study investigated the effects of temperature and immigration on AHL levels and biofouling in anaerobic membrane bioreactors. The hypothesis was that the immigrant microbial community would increase the AHL-mediated QS, thus stimulating biofouling and that low temperatures would exacerbate this. We observed that presence of immigrants, especially when exposed to low temperatures indeed increased AHL concentrations and fouling in the biofilms on the membranes. At low temperature, the concentrations of the main AHLs observed, *N*-dodecanoyl-L-homoserine lactone and *N*-decanoyl-L-homoserine lactone, were significantly higher in the biofilms than in the sludge and correlated significantly with the abundance of immigrant bacteria. Apparently low temperature, immigration and denser community structure in the biofilm stressed the communities, triggering AHL production and excretion. These insights into the social behaviour of reactor communities responding to low temperature and influx of immigrants have implications for biofouling control in bioreactors.



**Keywords:** fouling**,** quorum sensing, anaerobic membrane bioreactor, low-temperature effect, immigrant community effect


## 1. Introduction

Membrane bioreactors (MBR) are selected to treat wastewater when high-quality effluent is required. These systems retain high concentrations of bacteria (mixed liquor suspended solids) in the reactor, filtering the treated wastewater through a membrane (Meng et al.,

2017). However, the membranes are prone to fouling over time. Fouling occurs as foulants adhere to the membrane, forming a gel layer which facilitates biofilm formation on the surface of the membrane (Chen et al., 2020; Fortunato et al., 2017; Teng et al., 2020; Wu et al., 2020). MBR is expensive to operate due to cleaning requirements, the replacement of fouled membranes, increased energy requirements to force permeate through partially fouled membranes, and the need for gas sparging to help reduce fouling rates. These drawbacks limit their widespread use (Judd, 2017).

Biofilm formation on the surface of the membranes is regulated by quorum sensing (QS), a mechanism employed by bacteria to orchestrate communal behaviour in response to external environmental conditions and bacterial density (Papenfort and Bassler, 2016). Bacteria use various types and combinations of molecules to stimulate QS activity. In general, most of the Gram-negative QS bacteria use acyl homoserine lactones (AHL) for QS (Papenfort and Bassler, 2016). The AHL consists of an acyl chain of length between C4 - C18 attached to a homoserine lactone (HSL) ring; the acyl chain comes with or without "oxo" or "hydroxyl" groups at the C3 position (Milton et al., 2001). Numerous studies have highlighted the role of AHL in biofilm formation in aerobic systems, as well as the type of QS molecules secreted by pure cultures (Doberva et al., 2017; Naik et al., 2018). Since biofilm formation and biofouling have been shown to be related to the presence of AHL in aerobic MBR (Waheed et al., 2017), AHL have been successfully targeted to control biofilm formation and reduce biofouling in such systems (Iqbal et al., 2018). Unlike the physio-chemical strategies (Krzeminski et al., 2017; Rao et al., 2020; Tabraiz et al., 2017; Zeeshan et al., 2017), the biological strategies to regulate biofilm formation are mostly based on quorum quenching (QQ). This encompasses targeting the AHL molecules by adding QQ enzymes or adding the bacteria that produce those enzymes to lower AHL concentration (Kim et al., 2018).

While many studies have reported QS and QQ in aerobic treatment systems (including MBRs), studies focussing on QS and the role of AHL in anaerobic systems are scarce. One study has shown that the addition of AHL to an anaerobic reactor increased the size of the granules, and the concentration of the extracellular polymeric substances (EPSs) in the sample matrix (Ma et al., 2018b). Another study has characterized the role and types of AHL present in a granule-based anaerobic digester operating at mesophilic temperatures (Zhang et al., 2019). A recent study has reported AHL in the biofilm and sludge of AnMBR treating synthetic wastewater at 35 ℃ and demonstrated reduction of biofouling by quenching the AHL (Liu et al., 2019). Another study has reported the AHL types in AnMBR and upflow anaerobic sludge blanket with and without membrane at 15 ℃ (Tabraiz et al., 2020).

Anaerobic treatment is attracting increased attention as an alternative to energy-intensive aerobic systems as it recovers energy through methane production, thereby promoting carbon neutrality (Shamurad et al., 2020a; Shamurad et al., 2020b). Thus, many studies have recently been carried out to investigate the suitability of anaerobic MBR (AnMBR) to treat sewage and industrial wastewater to recover resources, but only a few studies have focused on the fouling of membranes in AnMBR (Jeong et al., 2017). Anaerobic wastewater treatment in low temperature regions is challenging as low temperature decreases anaerobic digestion rates (Maharaj and Elefsiniotis, 2001), which makes it paramount to prevent wash-out of crucial biomass and suggests that AnMBR could be the technology of choice. Recently, the importance of low-temperature carbon-neutral wastewater treatment, which can be facilitated by the introduction of a specialized inoculum has been highlighted for AnMBR (Petropoulos et al., 2021; Petropoulos et al., 2019) . Other studies, focussing on the fouling pattern in AnMBR operating between 25 ℃ and 10 ℃, reported increased fouling at low temperature (Watanabe et al., 2017). In addition, a recent study has reported that low temperature increased the fouling rates in aerobic MBR as well (Lee et al., 2018). However, no research

has focused on the fundamental mechanisms behind the occurrence of biofouling and biofilm formation at low temperature.

A recent study has reported that the exogenous (immigrant) community coming with real wastewater and temperature shift the microbial community of AnMBR (Seib et al., 2016). However, the study has not investigated its effect on fouling. The coexistence of biofouling causing bacteria with non-biofouling causing bacteria stimulated the AHL activity, which increased EPS and the fouling rates (~ 27 fold) in MBR (Ishizaki et al., 2017). Similarly, another study reported the competition through QS between two co-cultured bacterial strains; *Staphylococcus aureus* and *Pseudomonas aeruginosa.* The latter outcompeted the former using AHL-mediated QS (Smith et al., 2017). Therefore, we posit that the immigrant community can affect the QS activity in the AnMBR as it shall try to compete with the existing community, which possibly can affect the biofouling in the AnMBR.

In the present study, we hypothesized that low temperature and the presence of immigrant community from wastewater will affect the social behaviour of the community in AnMBR, and that this will be reflected by the presence and increased concentration of AHL quorum-sensing molecules. Moreover, the presence of high concentration of AHL shall be the cause of higher fouling rates at low temperature. To test these hypotheses two types of wastewater were employed; namely, sterilised sewage (without an immigrant community) and non-sterilised sewage (with an immigrant community) feeding AnMBR at two different temperatures (15 ℃ and 4 ℃). Subsequently, the status of AHL in the sludge and biofilm were analysed and compared. In addition, the SMP, microbial community in biofilm and sludge and fouling rates were monitored and compared.

## 2. Materials and methods

### 2.1 Reactor setup

Eight 1 L Quickfit® AnMBR reactors were operated at a hydraulic retention time (HRT) of 60 hours. To prevent acidification (accelerated hydrolysis/fermentation) in the absence of high numbers of methanogens and low fouling rate at 4 ℃, the HRT was kept relatively high. The reactors were equipped with hollow-fibre polyvinylidene difluoride (PVDF) membranes with a pore size of 0.1 μm (Zibo Yingxin Water Treatment Technology, China); the diameter of the fibres was 1.0 mm and membrane area in each reactor was 0.022 $m^2$. Organic loading rate was kept at 0.108 ± 0.01 $kg.m^{-3}.d^{-1}$. In the start of experiment, the influent and effluent of 0.4 $L.d^{-1}$ was maintained by a peristaltic pump (Watson-Marlow, UK) to achieve 0.75 $L.m^{-2}.hr^{-1}$ flux in all the reactors. To overcome the low flux at 4 ℃, due to higher permeate viscosity at low temperature, the pressure was increased by increasing the rpm of the peristaltic pump. All AnMBRs were operated at constant pressure mode throughout the experimentation. The membrane flux was estimated from the liquid volume of the effluent that passed through the membrane daily (24-hr period) for 110 days. The daily average flux reduction of the duplicate reactors was presented and compared to assess the fouling tendency at different reactors described above. The excess aqueous volume that remained in the AnMBR due to reduced flux (membrane fouling) was collected and centrifuged (4000 × *g* for 20 minutes); the solid part was returned to the reactor. The daily operation of reactors included 2 hours of relaxation (no flow for 30 minutes every 6 hours) and a 20-minute backwash period (once a day) with effluent (permeate) at the same flow rate (0.75 $L.m^{-2}.hr^{-1}$). Four reactors were placed at 4 ± 0.5 ℃, and the other four were placed at 15 ± 0.5 ℃ (Figure 1). At each temperature, two reactors were fed UV-sterilised sewage and two were fed non-sterile sewage. The reactors were stirred (4 cm x 0.5 cm stirrer at 70 rpm for 5 minutes, mixing intensity (G) = 25 $s^{-1}$, Gt = 15000) twice daily.

The reactors were inoculated (11.5 $g.L^{-1}$ of MLSS) with putatively cold adaptive biomass acclimated to 'cold' naturally (due to origin) and further acclimated to UV-sterile wastewater as substrate after subjected to numerous batches in an environmental lab (School of Engineering, Newcastle University, UK (Petropoulos et al., 2017). The cold adopted biomass was saved at 4 ℃. The anaerobic sludge was re-acclimatized on the above-mentioned conditions for 90 days prior the initiation of this experiment. Briefly, this biomass was originated from Lake Geneva N 46º 23' 04", E 6º 25' 07" (average temperature -16-6 ℃) and soils from Svalbard, in the high arctic from different points located at N 78º, E11,15,16º (average temperature -11-17 ℃).

## 2.2 Substrate

Primary settled sewage from the Tudhoe Mill wastewater treatment plant (Durham, UK) was used as substrate. The sewage was collected monthly and stored at 4 ℃ until use. The pH ranged between 6.7 and 7.3. The substrate (sewage) was sterilised with a UV lamp (Hozelock Vorton, UK) of 11W with the dose of 110 $KJ.cm^{-2}$, with successful sterilization tested and confirmed by the absence of colonies after spreading the sterilised sewage on nutrient and R2A agar plates (Sigma Aldrich, UK) as observed after five days incubation at 17 ± 2 ℃ (APHA, 2006). This sterilisation method was selected over conventional methods of autoclaving as it has less effect on the degradation of labile substrates in the sewage (Petropoulos et al., 2017).

## 2.3 Analytical methods

The reactors were monitored continuously for the operating parameters listed in Table S2. The sample collection time was selected as steady state conditions were evident for a prolong period (> 2 months). Biofilm from each AnMBR membrane was carefully scraped from the membrane surface on the $100^{th}$ day of the experiment with sterilised spatulas and weighed. 10 mL of mixed liquor (sludge) was also collected using a sterile 50 mL syringe. The reactors

were mixed to allow sludge suspension prior to collection. Chemical oxygen demand (COD) in the influent and effluent were measured based on APHA (2006). The MLSS and VSS content of the biomass was estimated gravimetrically (APHA, 2006).

### 2.4 EPS extraction

The collected biofilm was suspended in PBS (KCl; 0.2 g.L-1, NaCl; 8 g.L-1, $KH_2PO_4$; 0.24 g.L-1 $Na_2HPO_4$; 1.44 g.L-1) to make up to 10 mL volume. The suspension was vigorously shaken by hand to disperse the biofilm particles thoroughly. Biofilm and sludge (10 mL) samples were centrifuged at 6000 × g for 5 minutes (4 ℃). The supernatant was removed and filtered through a cellulose acetate 0.2 μm filter (Millipore, Merck). The filtrate represented the soluble microbial products (SMP)/soluble EPS. The sludge samples were then re-suspended in 10 mL PBS. This resuspension was sonicated for 2 minutes in Ultrasonic cleaner (USC-TH, VWR, UK), and then agitated in a shaker (KS400i IKA, UK) for 10 minutes at 150 rpm. The solution was further centrifuged at 8000 × g for 10 minutes in a 10 mL tube. The EPS present in the supernatant was defined as the loosely bound EPS (LB-EPS). For the tightly bound EPS (TB-EPS), the sludge pellets were re-suspended in 10 mL PBS, re-sonicated again for 3 minutes, then 2g of hydrated CER (cation exchange resin, Dowex® Marathon® C sodium form, Sigma Aldrich, Germany) was added to each 10 mL tube. The CER was washed twice with phosphate buffer (15min; 10 $mL \cdot g^{-1}$ Dowex) prior to use. The suspension was then centrifuged at 12000 × g for 30 minutes, and the EPS content of the separated supernatant was defined as the TB-EPS (Maqbool et al., 2015).

### 2.5 Protein and polysaccharide measurement

For the quantification of the total proteins present in the EPS samples, the Lowry method was used based on Folin-Ciocalteu phenolic reagent (Lowry et al., 1951), and colour intensity development at 750 nm (via a Spectramax M3 spectrophotometer ; Molecular Devices, USA). To measure the total polysaccharides, the phenol-sulphuric acid method was employed

(DuBois et al., 1956). A sample volume of 0.1 mL was taken and diluted with distilled water to a volume of 1 mL. 1 mL phenol solution (5%) was added to the sample tube, followed by 5 mL concentrated sulphuric acid (96%) (Sigma Aldrich, UK). The colour intensity of the solution was read in the spectrophotometer at 490 nm, the concentration was determined using a twelve-point standard curve of glucose from 0.125 to 200 $mg.L^{-1}$.

### 2.6 AHL extraction, identification and quantification

The AHL content of the biofilm and sludge samples was extracted using a modified Lade et al. (2014) method. The biofilm was dispersed in PBS (10 mL), centrifuged at 10000 × *g* for 10 minutes, the supernatant was separated and mixed with an equal volume of ethyl acetate. This mixture of the supernatant and ethyl acetate was agitated in a shaker (KS400i IKA, UK) at 180 rpm for 2 hours and allowed to separate on standing. The upper organic layer was harvested and then dried with $N_2$ gas (99.9%) purging. The dried residue was dissolved in a solution (0.5 mL) of acetonitrile and formic acid (0.1%) (Lade et al., 2014).

*N*-butanoyl-L-homoserine lactone (C4-HSL), *N*-3-oxo-butanoyl-L-homoserine lactone (3-oxo-C4- HSL), *N*-hexanoyl-L-homoserine lactone (C6-HSL), *N*-3-oxo-hexanoyl-L-homoserine lactone (3-oxo-C6-HSL), *N*-octonoyl-L-homoserine lactone (C8-HSL), *N*-3-oxo-octonoyl-L-homoserine lactone (3-oxo-C8-HSL), *N*-decanoyl-L-homoserine lactone (C10-HSL), *N*-3-oxo- decanoyl -L-homoserine lactone (3-oxo-C10-HSL), *N*-dodecanoyl-L-homoserine lactone (C12-HSL) and *N*-3-oxo-dodecanoyl-L-homoserine lactone (3-oxo-C12-HSL) were the main QS AHL molecules investigated (Table S3). The AHL were identified and quantified using ultra-performance liquid chromatography (Waters, UK) coupled with triple quadrupole mass spectrometry (UPLC-MS/MS) (Waters, Xevo TQ-S, UK), as described in the supplementary material (S1).

## 2.7 Molecular microbiological analysis

Genomic DNA extraction from biofilm and sludge samples was performed according to the modified protocol of Griffiths et al. (Griffiths et al., 2000), as described in the supplementary material (S2). The quality and concentration of the DNA samples were measured using a Nanodrop spectrophotometer (Thermo Fisher, UK) as described previously (Shamurad et al., 2019a).

## 2.8 *16S rRNA gene Sequencing*

Polymerase chain reaction (PCR) amplification of the DNA extracted prior to sequencing involved the universal reverse primer 806R (GGACTACHVGGGTWTCTAAT) and the forward primer 515F (GTGCCAGCMGCCGCGGTAA) targeting the V4 16S rRNA gene (Kozich et al., 2013). PCR amplification was performed with GoTaq® Hot Start master mix (ThermoFisher, UK) under the following conditions: initial denaturation (94 ℃, 3 min), denaturation 35 cycles (94 ℃, 45 sec), annealing (50 ℃, 30 sec ), extension (70 ℃, 90 sec). Quality control was carried out by checking for fragments of the correct size using an agarose gel electrophoresis check; library preparation included tagging; equal concentrations of all samples were mixed and cleaned-up. After amplification, sequencing was carried out using an Illumina MiSeq V2 (2 × 250 bp) to identify the 16S rDNA amplicons.

The raw sequence data (FastQ files) obtained from sequencing (Illumina MiSeq) was de-multiplexed, quality filtered and binned into amplicon sequence variant (ASV) using DADA2 (Callahan et al., 2016; Shamurad et al., 2019b) default parameters in the QIIME2 pipeline (Caporaso et al., 2010). The taxonomical assignment was then accomplished using the MIDAS 2.0 database, and a feature table was produced containing the ASVs and their abundance per each sequenced DNA sample, this feature table was used for data visualization and statistical analysis.

### 2.9 Co-occurrence between AHL concentration and microbial taxa

A correlation matrix was developed by calculating all possible pairwise Pearson correlations among the microbial community (genus level), and AHLs present in samples from the study (n = 16). A correlation between two items was considered if the Pearson correlation coefficient was $\geq 0.7$, and the *p*-value was $\leq 0.05$. To reduce the chances of obtaining false-positive results, the *p*-values were adjusted with a multiple testing correction using the Benjamini–Hochberg method (Benjamini and Hochberg, 1995). The pairwise correlations of the bacterial genus and AHL formed their co-occurrence networks. Network analyses were performed in R environment and was further visualized and explored to identify its topological properties (i.e., clustering coefficient, shortest average path length and modularity) in Gephi (Bastian et al., 2009).

### 2.10 Data visualization and statistical analysis

Principal component analysis of the microbial communities in biofilm and sludge of all reactors was performed using phyloseq package (McMurdie and Holmes, 2013). The data of community abundance, proteins/polysaccharides and AHL concentration were correlated and visualized using microbiome package in R following the procedures described elsewhere (Shamurad et al., 2019a; Shamurad et al., 2020c; Shamurad et al., 2020d). Analysis of variance (ANOVA) in R was conducted to evaluate the effect of temperature and feed type on AHL concentration in sludge and biofilm. T-test was performed to see if the biofilm formation and flux reduction at different conditions were significant or not.

## 3. Results

### 3.1 AHL profiles

The present study evaluated the presence and abundance of 10 specific AHL in both the sludge and the biofilm of eight AnMBR operated under different conditions (4 ℃ and 15 ℃,

sterile and non-sterile). Overall, seven AHL were detected in both the biofilm and the sludge at both temperatures and treatments, viz.: C4-HSL, 3-oxo-C4- HSL, C8- HSL, C10- HSL, 3-oxo-C10- HSL, C12- HSL and 3-oxo-C12- HSL. The AHL with the highest concentrations in the biofilm were C12- HSL, C10- HSL and C4- HSL. Their concentrations differed with temperature and type of feed (sterilised or non-sterilised sewage). The most striking differences appeared in the 4 ℃ biofilms, where high concentrations of long-chain AHL (C10-HSL, C12-HSL) were observed compared to biofilms at 15 ℃ (Figure 2). Comparable concentration of the AHL were

### 3.2 Effect of temperature on AHL in biofilm

Biofilms that developed in the AnMBR fed with non-sterilised sewage at low temperature (4 ℃) (AnMBR_B 4 ℃) had the highest concentrations of C12-HSL (74.2 ± 16.2 µg.kg$^{-1}$ biofilm) and C10-HSL (14.9 ± 5.1 µg.kg$^{-1}$ biofilm), whilst in those operating at 15 ℃ (AnMBR_B 15 ℃) C12-HSL was absent or negligible (0-19 ng. kg$^{-1}$ biofilm). In those operating at 15 ℃, C10-HSL was the most prevalent AHL (1225 ± 65.7 ng.kg$^{-1}$ biofilm), followed by C4-HSL (428 ± 35 ng.kg$^{-1}$ biofilm) and C8-HSL (232 ± 86 ng.kg$^{-1}$ biofilm). Other AHL molecules were found at low concentrations (0-160 ng.kg$^{-1}$ biofilm) in all the biofilm samples regardless of the operational temperature. The biofilms of the AnMBR operating at 4 ℃ fed with sterilised sewage (sAnMBR_B 4 ℃) contained the highest concentration (2510 ± 621 ng.kg$^{-1}$ biofilm) of C10-HSL followed by C12-HSL (1234 ± 891 ng.kg$^{-1}$ biofilm) and C4-HSL (799 ± 488 ng.kg$^{-1}$ biofilm). The concentrations of 3-oxo-C4-HSL (308 ± 96 ng.kg$^{-1}$ biofilm), C8-HSL (301 ± 120 ng.kg$^{-1}$ biofilm), 3-oxo-C10-HSL (8.9 ng.kg$^{-1}$ biofilm) and 3-oxo-C12-HSL (8.6 ng.kg$^{-1}$ biofilm) were found at comparatively lower concentrations. The biofilm in the AnMBR fed with sterilised sewage at 15 $^{O}$C (sAnMBR_B 15 ℃) showed the highest concentration of C10- HSL (1290 ± 362 ng.kg$^{-1}$ biofilm), followed by 3-oxo-C4-HSL (324 ±112 ng.kg$^{-1}$ biofilm), C8- HSL (540 ng.kg$^{-1}$ biofilm) and C4-HSL

(259 ± 56 ng.kg$^{-1}$ biofilm). Thus, at lower temperature (4 ℃), the C10-HSL, C4-HSL concentrations in the biofilm were two to three times higher than at the higher temperature (15 ℃) (Figure 2).

### 3.3 Effect of feed type (sterile and non- sterile sewage) on AHL in biofilms

The type of sewage feed had a substantial effect on the AHL concentrations in the 4 ℃ reactors, especially in the biofilms. The C10- HSL and C12- HSL concentrations were respectively six and seventy times lower in sAnMBR_B 4 ℃ (fed sterile wastewater/no immigrant) than in the AnMBR_B 4 $^{O}$C (fed non-sterile sewage/with immigrants). In contrast, the concentration of small and medium-chain AHL were higher in the sAnMBR_B 4 ℃; C4-HSL (6 times), 3-oxo-C4- HSL (2 times), C8- HSL (3 times). At higher temperature (15 ℃) the difference in the AHL concentrations found in the biofilms of systems fed with sterilised versus non-sterilised wastewater was minimal (Figure 2).

### 3.4 Effect of the feed type and temperature on AHL in sludge

AHL concentrations in the sludge were low compared to the biofilms at the corresponding temperature and type of feed sewage. They ranged between 0 - 113 ng.L$^{-1}$ (Figure 2). No significant differences were observed in the concentrations of the AHL in the sludge between the different temperatures or sewage feeds.

Analysis of variance (ANOVA), two-factor with replication, revealed that the temperature ($p < 0.05$, F =18.4, $F_{crit}$ = 7.7) and the type of feed sewage ($p < 0.05$, F = 15.8, $F_{crit}$ = 7.7), both affected the concentration of the AHL (total concentration of 7 AHL) significantly in the biofilms. Furthermore, ANOVA showed that the extent of the effect of both factors, i.e. temperature and feed type, on the AHL concentrations was not equal. Temperature affected the AHL status more significantly than the wastewater feed type (immigrant community) ($p_{temperature} < p_{feed}$), but both were instrumental in the biofilm QS activity through AHL. On

292 the contrary, ANOVA revealed that neither the temperature nor the type of wastewater feed
293 affected sludge AHL concentration significantly (total of all AHL) ($p > 0.05$).

294 **3.5 Protein & polysaccharide correlations with AHL, and membrane fouling**

295 The biofilm and the sludge of reactors fed with non-sterile wastewater (with immigrant) had
296 higher concentrations of proteins and polysaccharides compared to the reactors fed with
297 sterilised wastewater (no immigrants). In addition, higher temperatures resulted in reduced
298 levels of proteins and polysaccharides in the biofilms, but not in the sludge where protein
299 concentrations were higher than in the lower temperature reactors (Figure S1b). This may be
300 related to the low concentration of C4-HSL and the absence of C8-HSL in one of the non-
301 sterile wastewater fed reactors at 4 ℃ (Figure 2), as C4-HSL was significantly correlated
302 (Spearman's coefficient $\rho > 0.9$, $p < 0.05$) with proteins at 15 ℃. Furthermore, at 4 ℃,
303 proteins and polysaccharides were significantly (Spearman's coefficient $\rho > 0.9$, $p < 0.05$)
304 correlated with C10-HSL, C12-HSL and total AHL. The positive correlation between
305 proteins/polysaccharides and other AHL was also found; however, although apparent, this
306 correlation was not statistically significant ($p > 0.05$) (Figure 3).

307 Biofouling occurred under all conditions, but was more pronounced at the lower temperature,
308 especially in the reactors fed non-sterile wastewater (Figure S2): reduction in membrane flux
309 was almost 2-fold higher for the AnMBR fed with non-sterile sewage compared to the reactor
310 with sterile feed at 4 ℃ (Figure S2 a). Higher fouling rates are commonly associated with the
311 higher levels of proteins and polysaccharides, which was the most likely cause of higher
312 fouling rates in the AnMBR_B at 4 ℃. The higher levels of AHL, especially long-chain AHL
313 (C10-HSL, C12-HSL) in the AnMBR_B at 4 ℃ were correlated significantly with the levels
314 of proteins and polysaccharides. With sterile feed, fouling appeared unaffected by
315 temperature. Though percentage flux reduction showed that fouling tends to be higher at
316 sterile fed AnMBR at 4 ℃ but not significant. Similarly, the biofilm formation tends to be

317 higher at sterile fed AnMBR at 4 ℃ (Figure 4). This is supported by the status of the AHL
318 observed in biofilm under these conditions. For the non-sterile feed reactors, fouling was only
319 pronounced at the lower temperature (4 ℃), a phenomenon that was expected considering the
320 status not only of the AHL but also of the proteins and polysaccharides concentration which
321 were higher under those conditions. Similarly, biofilm per unit area was highest in the non-
322 sterile fed AnMBR_4C (Figure 4).

323 Few studies have reported similar type of AHL in anaerobic/anoxic membrane bioreactors (Li
324 et al., 2019). Therefore, AHL were quenched using anaerobic quorum quenching bacteria to
325 reduce the biofouling in AnMBR treating synthetic wastewater (Liu et al., 2019). Similarly, a
326 recent study reported the consortium of facultative AHL quenching bacteria to reduce the
327 fouling in AnMBR (Xu et al., 2020). The AHL types found in current study can be targeted
328 for the fouling reduction in these conditions (low temperature) to make AnMBR sustainable.

329 **3.6 Microbial community composition and their correlation with AHL**

330 The archeal and bacterial community structure of biofilm and sludge varied with temperature
331 and feed type (Figure 5 a, b & c). Canonical correlation analysis (CCA) was carried out to
332 find the correlation between the core communities (most abundant 30 genera) for both
333 bacteria and archaea of the reactor sludge and biofilm, and the AHL. The C12-HSL, C10-
334 HSL, 3-oxo-C10-HSL and C4-HSL were positively correlated (Figure S5) with the
335 predominant hydrogenotrophic methanogenic archaea which were abundant at 4 ℃;
336 *Methanobacterium, Methanosarcina, Methanobrevibacter, Methanosphaerula and*
337 *Methanospirillum.* Previous studies (Zhang et al., 2012) have reported *Methanosaeta*
338 *harundinacea, Methanobacterium formicicum, Methanobacterium thermautotrophicus* and
339 *Methanosarcina mazei* as key archaeal genera and species linked to the production of AHL
340 (carboxylated-AHL) in pure culture, showing some similarity with the current study. A recent
341 study (Zhang et al., 2019) reported the presence of QS molecules, including C10-HSL, C12-

342 HSL, in mesophilic anaerobic digesters, but no previous studies have focused on AHL status
343 in low temperature (< 37 ℃) anaerobic reactors, where fouling and operational challenges
344 (i.e. lower process rates) are more evident (Petropoulos et al., 2020; Petropoulos et al., 2019).

345 In the case of bacteria, the relative abundances of *Synergistaceae*, *Anaerolineaceae (T78),*
346 *Anaerovorax, Brachy, Trichococcus, Bacteroidetes (SHA.94) and Rhodocyclaceae* were
347 higher at 4 ℃ compared to 15 ℃ and higher in biofilms compared to sludge and were
348 correlated with 3-oxo-C10-HSL, C12-HSL and C8-HSL (Figure S5). Furthermore,
349 *Romboutsia* has recently been reported as a taxon responsible for QS through AI-2 (4,5-
350 Dihydroxy-2,3 pentanedione) (Gerritsen et al., 2019), but not through AHL. Similarly,
351 species from the genus *Clostridium* have been reported as using auto inducer peptides as QS
352 molecules for spore formation and exotoxins excretion (Li et al., 2011; Steiner et al., 2012).
353 An OTU of *Christensenellaceae* showing correlation with C10-HSL and C8-HSL has been
354 previously reported (Ma et al., 2018a).

355 Thus, it can be concluded that temperature shaped the community and affected the QS
356 activity. Though, this was not the case for the sludge biomass, as the community structure
357 varied but the AHL molecules concentration did not ($p > 0.05$). One can argue that physical,
358 chemical and biological conditions were different in the biofilm and the sludge, the former
359 producing a denser community structure and a reduced affinity for substrate, leading to
360 bacterial starvation (mainly due to limited hydrolysis (Petropoulos et al., 2019)). Particularly
361 at low temperatures, starvation seems inevitable as the availability for substrates is expected
362 reduced (Nedwell, 1999), which was the case in the current study (Figure S7). Such
363 starvation phenomena can be aligned with hydrogenotrophic methanogenesis and could lead
364 to high concentrations (8.61-14.28 $\mu g.L^{-1}$) of C12-HSL (Zhang et al., 2019). Presuming
365 starvation conditions, bacteria tend to produce glucose-dominated EPS when subjected to
366 such conditions (Myszka and Czaczyk, 2009), hypothesis also observed in the current study

(Figure S1 ). Therefore, we posit that cellular density, starvation and low temperature collectively increased the environment stress level in the biofilms, eliciting a clear response in AHL signature. Thus, at the lower temperature (4 ℃) a particular community evolved and survived through quorum sensing using long-chain AHL, especially C10-HSL and C12-HSL, as autoinducers, and subsequently excreted higher concentrations of polysaccharides and proteins which also caused higher fouling rates. Since polysaccharides constitute a significant component of EPS, they play a major role in membrane fouling, especially at low temperatures (Ma et al., 2013).

### 3.7 Immigrant and emigrant communities and their correlation & co-occurrence with AHL

The effect of temperature on the AHL concentration in biofilms from the sterilised sewage-fed AnMBR was minor compared to its effect on the AHL concentration in biofilm from AnMBR fed with non-sterilised wastewater. This was probably due to the 'immigrating' species present in the latter influent striving to adapt to the new environment and starting to compete with the established inoculated community in the reactors. Interestingly, the question arises as to why the immigration did not affect the QS activity significantly in the sludge of these reactors?

The immigrant community was represented by the amplicon sequence variants (ASVs) present exclusively in reactors fed with non-sterilised sewage, and absent from the reactors fed sterilised sewage of the same temperature (Figure 6, Figure S3), whereas emigrants were represented by ASVs present only in the reactors fed with sterilised sewage, and absent from reactors with a non-sterilised feed (Figure S4, Figure S3). Additionally, the immigrants were also traced in influent (non-sterile sewage) microbial community (Table S4, Table S5). Majority of the immigrant genus were found in the influent wastewater samples analysed.

Methylocaldum was the most dominant genus immigrating into the reactors at both temperatures (Figure 6). We also conducted the co-occurrence network analysis to determine groups of bacteria positively correlated with the AHL (Pearson's $R > 0.7$, $p < 0.05$), highlighting the immigrants and emigrants bacteria. The co-occurrence network consists of 621 nodes (614 taxa and 7 AHLs) and 9009 edges with an average degree or node connectivity of 28.577. The average network distance between all pairs of nodes (average path length) was 4.185 edges with a network diameter of 12 edges. As shown in Figure 7, network analysis produces 6 bacterial modules (or cluster). The short-chain AHL (C4-HSL, 3-oxo-C4-HSL, C8-HSL, 3-oxo-C8-HSL) exhibit no apparent module classification. However, long-chain AHL (C10-HSL, 3-oxo-C10-HSL, C12-HSL, 3-oxo-C12-HSL) are highly associated in module VI, which is dominated by immigrant bacteria.

In the low-temperature reactors, biofilms and sludge had lower richness than the higher temperature reactors. For emigrants, the biofilms contained a relatively lower abundance of emigrants than the sludge, like immigrants (Figure S6a & b). The richness of the emigrant cohort in the lower temperature reactor was higher than in higher temperature reactors. Interestingly, the lower temperature reactors fed sterilised sewage had higher richness in the biofilm and sludge compared to the reactors with non-sterilised feed; and vice versa in case of richness higher temperature reactors (Figure S6 c). It indicates that challenging conditions prevailed at the lower temperature compared to the higher temperature, and in the biofilms compared to the sludge, where selective species can cope. Low richness has been explicitly reported in challenging environmental conditions (Walsh et al., 2005; Zhou et al., 2016). Immigration caused a change in the community and resulted in distinct trends in numbers within the immigrant and emigrant communities, especially at 4 ℃, and most clearly within the membrane biofilm. The immigration of non- or poorly adapted biomass at low temperature, especially biofilm (stressful conditions) resulted in high QS activity mediated

through AHL due to low-temperature stress. We consider that the higher density of microbes (Moreno-Gámez et al., 2017) and thus, higher competition for substrate, higher starvation level (Lazazzera, 2000; Liu et al., 2016) and high transmembrane pressure led to environmental stress in the biofilm relative to the suspended sludge, especially at the lower temperature, which caused the high QS activity (Cornforth and Foster, 2013; Shen et al., 2019). Additionally, significant correlation ($p < 0.05$) of immigrants with the long-chain AHL strengthens the argument that high QS activity occurs in low-temperature reactor biofilms due to immigrant competition mediated by long-chain AHL, especially C10-HSL and C12-HSL (Figure 7). A recent study also proved that *P. aeruginosa* outcompeted the *Staphylococcus aureus* using 3-oxo-C12-HSL (long-chain AHL) (Smith et al., 2017).

Bioreactors and biofilms are complex ecosystems, and different factors can shift the community structure as well as affect the inter and intra-species communication. This study has shown how the concentration of QS molecules reflects operating conditions and biofouling processes, but more studies on single and multiple species with controlled conditions are required to understand the behaviour of biofilms in AnMBR affected by a more extensive range of environmental variables. In addition, current study was conducted at low flux (0.75 $L.m^{-2}.hr^{-1}$), studies on higher flux are recommended to evlaluate the fouling patterens properly.

## 4. Conclusions

Biofilm formation and biofouling correlated with elevated levels of quorum sensing AHL molecules in the biofilm; AHLs were present at far lower concentrations in the sludge. Highest levels of C10-HSL and C12-HSL were observed in biofilms of reactors fed non-sterile sewage at low temperature, probably due to immigration-related stress. At the higher operating temperature (15 ℃), the AHL levels were less, as competition and stress were

reduced due to the less challenging temperature. The study suggests potential mechanisms for future QS based manipulation and shaping of biofilms in AnMBRs to mitigate membrane fouling.

**Acknowledgements**

We gratefully acknowledge funding from Commonwealth Scholarship Commission in UK and Newcastle University UK; Evangelos Petropoulos and Jan Dolfing acknowledge BB/K003240/1 (Engineering synthetic microbial communities for biomethane production).

**References**

APHA, W., 2006. Standart Methods for Examination of Water and Wastewater, 19th ed. ed. Washington DC: American Public Heatth Association.

Bastian, M., Heymann, S., Jacomy, M., 2009. International AAAI Conference on Weblogs and Social Media. 2009, Gephi: an open source software for exploring and manipulating networks, pp. 361-362.

Benjamini, Y., Hochberg, Y., 1995. Controlling the false discovery rate: a practical and powerful approach to multiple testing. Journal of the Royal Statistical Society: series B (Methodological) 57, 289-300.

Callahan, B.J., McMurdie, P.J., Rosen, M.J., Han, A.W., Johnson, A.J.A., Holmes, S.P., 2016. DADA2: high-resolution sample inference from Illumina amplicon data. Nature Methods 13, 581–583.

Caporaso, J.G., Kuczynski, J., Stombaugh, J., Bittinger, K., Bushman, F.D., Costello, E.K., Fierer, N., Pena, A.G., Goodrich, J.K., Gordon, J.I., 2010. QIIME allows analysis of high-throughput community sequencing data. Nature methods 7, 335.

Chen, Y., Shen, L., Li, R., Xu, X., Hong, H., Lin, H., Chen, J., 2020. Quantification of interfacial energies associated with membrane fouling in a membrane bioreactor by using BP and GRNN artificial neural networks. Journal of Colloid and Interface Science 565, 1-10.

Cornforth, D.M., Foster, K.R., 2013. Competition sensing: the social side of bacterial stress responses. Nature Reviews Microbiology 11, 285–293.

Doberva, M., Stien, D., Sorres, J., Hue, N., Sanchez-Ferandin, S., Eparvier, V., Ferandin, Y., Lebaron, P., Lami, R., 2017. Large Diversity and Original Structures of Acyl-Homoserine Lactones in Strain MOLA 401, a Marine Rhodobacteraceae Bacterium. Frontiers in Microbiology 8, 1152.

DuBois, M., Gilles, K.A., Hamilton, J.K., Rebers, P.A., Smith, F., 1956. Colorimetric method for determination of sugars and related substances. Analytical Chemistry 28, 350-356.

Fortunato, L., Qamar, A., Wang, Y., Jeong, S., Leiknes, T., 2017. In-situ assessment of biofilm formation in submerged membrane system using optical coherence tomography and computational fluid dynamics. Journal of Membrane Science 521, 84-94.

Gerritsen, J., Hornung, B., Ritari, J., Paulin, L., Rijkers, G.T., Schaap, P.J., De Vos, W.M., Smidt, H., 2019. A comparative and functional genomics analysis of the genus Romboutsia provides insight into adaptation to an intestinal lifestyle. BioRxiv, 845511.

Griffiths, R.I., Whiteley, A.S., O'Donnell, A.G., Bailey, M.J., 2000. Rapid method for coextraction of DNA and RNA from natural environments for analysis of ribosomal DNA- and rRNA-based microbial community composition. Applied and Environmental Microbiology 66, 5488-5491.
Iqbal, T., Lee, K., Lee, C.-H., Choo, K.-H., 2018. Effective quorum quenching bacteria dose for anti-fouling strategy in membrane bioreactors utilizing fixed-sheet media. Journal of Membrane Science 562, 18-25.
Ishizaki, S., Sugiyama, R., Okabe, S., 2017. Membrane fouling induced by AHL-mediated soluble microbial product (SMP) formation by fouling-causing bacteria co-cultured with fouling-enhancing bacteria. Scientific Reports 7, 1-8.
Jeong, Y., Hermanowicz, S.W., Park, C., 2017. Treatment of food waste recycling wastewater using anaerobic ceramic membrane bioreactor for biogas production in mainstream treatment process of domestic wastewater. Water Research 123, 86-95.
Judd, S.J., 2017. Membrane technology costs and me. Water Research 122, 1-9.
Kim, T.H., Lee, I., Yeon, K.-M., Kim, J., 2018. Biocatalytic membrane with acylase stabilized on intact carbon nanotubes for effective antifouling via quorum quenching. Journal of Membrane Science 554, 357-365.
Kozich, J.J., Westcott, S.L., Baxter, N.T., Highlander, S.K., Schloss, P.D., 2013. Development of a dual-index sequencing strategy and curation pipeline for analyzing amplicon sequence data on the MiSeq Illumina sequencing platform. Applied and Environmental Microbiology 79, 5112-5120.
Krzeminski, P., Leverette, L., Malamis, S., Katsou, E., 2017. Membrane bioreactors–a review on recent developments in energy reduction, fouling control, novel configurations, LCA and market prospects. Journal of Membrane Science 527, 207-227.
Lade, H., Paul, D., Kweon, J.H., 2014. Isolation and molecular characterization of biofouling bacteria and profiling of quorum sensing signal molecules from membrane bioreactor activated sludge. International Journal of Molecular Mciences 15, 2255-2273.
Lazazzera, B.A., 2000. Quorum sensing and starvation: signals for entry into stationary phase. Current Opinion in Microbiology 3, 177-182.
Lee, K., Park, J.-S., Iqbal, T., Nahm, C.H., Park, P.-K., Choo, K.-H., 2018. Membrane biofouling behaviors at cold temperatures in pilot-scale hollow fiber membrane bioreactors with quorum quenching. Biofouling 34, 912-924.
Li, J., Chen, J., Vidal, J.E., McClane, B.A., 2011. The Agr-like quorum-sensing system regulates sporulation and production of enterotoxin and beta2 toxin by Clostridium perfringens type A non-food-borne human gastrointestinal disease strain F5603. Infection and Immunity 79, 2451-2459.
Li, T., Guo, F., Lin, Y., Li, Y., Wu, G., 2019. Metagenomic analysis of quorum sensing systems in activated sludge and membrane biofilm of a full-scale membrane bioreactor. Journal of Water Process Engineering 32, 100952.
Liu, J., Eng, C.Y., Ho, J.S., Chong, T.H., Wang, L., Zhang, P., Zhou, Y., 2019. Quorum quenching in anaerobic membrane bioreactor for fouling control. Water Research 156, 159-167.
Liu, X., Sun, S., Ma, B., Zhang, C., Wan, C., Lee, D.-J., 2016. Understanding of aerobic granulation enhanced by starvation in the perspective of quorum sensing. Applied Microbiology and Biotechnology 100, 3747-3755.
Lowry, O.H., Rosebrough, N.J., Farr, A.L., Randall, R.J., 1951. Protein measurement with the Folin phenol reagent. Journal of biological chemistry 193, 265-275.
Ma, C., Yu, S., Shi, W., Heijman, S., Rietveld, L., 2013. Effect of different temperatures on performance and membrane fouling in high concentration PAC–MBR system treating micro-polluted surface water. Bioresource Technology 141, 19-24.

Ma, H., Ma, S., Hu, H., Ding, L., Ren, H., 2018a. The biological role of N-acyl-homoserine lactone-based quorum sensing (QS) in EPS production and microbial community assembly during anaerobic granulation process. Scientific Reports 8, 15793.
Ma, H., Wang, X., Zhang, Y., Hu, H., Ren, H., Geng, J., Ding, L., 2018b. The diversity, distribution and function of N-acyl-homoserine lactone (AHL) in industrial anaerobic granular sludge. Bioresource Technology 247, 116-124.
Maharaj, I., Elefsiniotis, P., 2001. The role of HRT and low temperature on the acid-phase anaerobic digestion of municipal and industrial wastewaters. Bioresource Technology 76, 191-197.
Maqbool, T., Khan, S.J., Waheed, H., Lee, C.-H., Hashmi, I., Iqbal, H., 2015. Membrane biofouling retardation and improved sludge characteristics using quorum quenching bacteria in submerged membrane bioreactor. Journal of Membrane Science 483, 75-83.
McMurdie, P.J., Holmes, S., 2013. phyloseq: an R package for reproducible interactive analysis and graphics of microbiome census data. PloS One 8, e61217.
Meng, F., Zhang, S., Oh, Y., Zhou, Z., Shin, H.-S., Chae, S.-R., 2017. Fouling in membrane bioreactors: an updated review. Water Research 114, 151-180.
Milton, D.L., Chalker, V.J., Kirke, D., Hardman, A., Cámara, M., Williams, P., 2001. The LuxM Homologue VanM from Vibrio anguillarumDirects the Synthesis of N-(3-Hydroxyhexanoyl) homoserine Lactone and N-Hexanoylhomoserine Lactone. Journal of Bacteriology 183, 3537-3547.
Moreno-Gámez, S., Sorg, R.A., Domenech, A., Kjos, M., Weissing, F.J., Van Doorn, G.S., Veening, J.-W., 2017. Quorum sensing integrates environmental cues, cell density and cell history to control bacterial competence. Nature Communications 8, 1-12.
Myszka, K., Czaczyk, K., 2009. Characterization of adhesive exopolysaccharide (EPS) produced by Pseudomonas aeruginosa under starvation conditions. Current Microbiology 58, 541-546.
Naik, M.M., Naik, S.P., Dubey, S.K., Bhat, C., Charya, L.S., 2018. Enhanced exopolysaccharide production and biofilm forming ability in methicillin resistant Staphylococcus sciuri isolated from dairy in response to acyl homoserine lactone (AHL). Journal of food science and technology 55, 2087-2094.
Nedwell, D.B., 1999. Effect of low temperature on microbial growth: lowered affinity for substrates limits growth at low temperature. FEMS microbiology ecology 30, 101-111.
Papenfort, K., Bassler, B.L., 2016. Quorum sensing signal–response systems in Gram-negative bacteria. Nature Reviews Microbiology 14, 576-587.
Petropoulos, E., Dolfing, J., Davenport, R.J., Bowen, E.J., Curtis, T.P., 2017. Developing cold-adapted biomass for the anaerobic treatment of domestic wastewater at low temperatures (4, 8 and 15 C) with inocula from cold environments. Water research 112, 100-109.
Petropoulos, E., Shamurad, B., Acharya, K., Tabraiz, S., 2020. Domestic wastewater hydrolysis and lipolysis during start-up in anaerobic digesters and microbial fuel cells at moderate temperatures. International Journal of Environmental Science and Technology 17, 27-38.
Petropoulos, E., Shamurad, B., Tabraiz, S., Yu, Y., Davenport, R., Curtis, T.P., Dolfing, J., 2021. Sewage treatment at 4° C in anaerobic upflow reactors with and without a membrane–performance, function and microbial diversity. Environmental Science: Water Research & Technology 7, 156-171.
Petropoulos, E., Yu, Y., Tabraiz, S., Yakubu, A., Curtis, T.P., Dolfing, J., 2019. High rate domestic wastewater treatment at 15° C using anaerobic reactors inoculated with cold-adapted sediments/soils–shaping robust methanogenic communities. Environmental Science: Water Research & Technology 5, 70-82.

Rao, L., Tang, J., Hu, S., Shen, L., Xu, Y., Li, R., Lin, H., 2020. Inkjet printing assisted electroless Ni plating to fabricate nickel coated polypropylene membrane with improved performance. Journal of Colloid and Interface Science 565, 546-554.
Seib, M., Berg, K., Zitomer, D., 2016. Influent wastewater microbiota and temperature influence anaerobic membrane bioreactor microbial community. Bioresource Technology 216, 446-452.
Shamurad, B., Gray, N., Petropoulos, E., Dolfing, J., Quintela-Baluja, M., Bashiri, R., Tabraiz, S., Sallis, P., 2020a. Low-temperature pretreatment of organic feedstocks with selected mineral wastes sustains anaerobic digestion stability through trace metal release. Environmental Science & Technology 54, 9095-9105.
Shamurad, B., Gray, N., Petropoulos, E., Tabraiz, S., Acharya, K., Quintela-Baluja, M., Sallis, P., 2019a. Co-digestion of organic and mineral wastes for enhanced biogas production: reactor performance and evolution of microbial community and function. Waste Management 87, 313-325.
Shamurad, B., Gray, N., Petropoulos, E., Tabraiz, S., Acharya, K., Quintela-Baluja, M., Sallis, P., 2019b. Data of metal and microbial analyses from anaerobic co-digestion of organic and mineral wastes. Data in brief 24, 103934.
Shamurad, B., Gray, N., Petropoulos, E., Tabraiz, S., Membere, E., Sallis, P., 2020b. Predicting the effects of integrating mineral wastes in anaerobic digestion of OFMSW using first-order and Gompertz models from biomethane potential assays. Renewable Energy 152, 308-319.
Shamurad, B., Gray, N., Petropoulos, E., Tabraiz, S., Sallis, P., 2020c. Improving the methane productivity of anaerobic digestion using aqueous extracts from municipal solid waste incinerator ash. Journal of environmental management 260, 110160.
Shamurad, B., Sallis, P., Petropoulos, E., Tabraiz, S., Ospina, C., Leary, P., Dolfing, J., Gray, N., 2020d. Stable biogas production from single-stage anaerobic digestion of food waste. Applied Energy 263, 114609.
Shen, P., Lees, J.A., Bee, G.C.W., Brown, S.P., Weiser, J.N., 2019. Pneumococcal quorum sensing drives an asymmetric owner–intruder competitive strategy during carriage via the competence regulon. Nature Microbiology 4, 198-208.
Smith, A.C., Rice, A., Sutton, B., Gabrilska, R., Wessel, A.K., Whiteley, M., Rumbaugh, K.P., 2017. Albumin inhibits Pseudomonas aeruginosa quorum sensing and alters polymicrobial interactions. Infection and Immunity 85, e00116-00117.
Steiner, E., Scott, J., Minton, N.P., Winzer, K., 2012. An agr quorum sensing system that regulates granulose formation and sporulation in Clostridium acetobutylicum. Appl. Environ. Microbiol. 78, 1113-1122.
Tabraiz, S., Haydar, S., Sallis, P., Nasreen, S., Mahmood, Q., Awais, M., Acharya, K., 2017. Effect of cycle run time of backwash and relaxation on membrane fouling removal in submerged membrane bioreactor treating sewage at higher flux. Water Science and Technology 76, 963-975.
Tabraiz, S., Shamurad, B., Petropoulos, E., Charlton, A., Mohiudin, O., Danish Khan, M., Ekwenna, E., Sallis, P., 2020. Diversity of Acyl Homoserine Lactone Molecules in Anaerobic Membrane Bioreactors Treating Sewage at Psychrophilic Temperatures. Membranes 10, 320.
Teng, J., Wu, M., Chen, J., Lin, H., He, Y., 2020. Different fouling propensities of loosely and tightly bound extracellular polymeric substances (EPSs) and the related fouling mechanisms in a membrane bioreactor. Chemosphere, 126953.
Waheed, H., Xiao, Y., Hashmi, I., Stuckey, D., Zhou, Y., 2017. Insights into quorum quenching mechanisms to control membrane biofouling under changing organic loading rates. Chemosphere 182, 40-47.

Walsh, D.A., Papke, R.T., Doolittle, W.F., 2005. Archaeal diversity along a soil salinity gradient prone to disturbance. Environmental Microbiology 7, 1655-1666.
Watanabe, R., Nie, Y., Wakahara, S., Komori, D., Li, Y.-Y., 2017. Investigation on the response of anaerobic membrane bioreactor to temperature decrease from 25° C to 10° C in sewage treatment. Bioresource Technology 243, 747-754.
Wu, M., Chen, Y., Lin, H., Zhao, L., Shen, L., Li, R., Xu, Y., Hong, H., He, Y., 2020. Membrane fouling caused by biological foams in a submerged membrane bioreactor: mechanism insights. Water Research, 115932.
Xu, B., Ng, T.C.A., Huang, S., Shi, X., Ng, H.Y., 2020. Feasibility of isolated novel facultative quorum quenching consortiums for fouling control in an AnMBR. Water Research 169, 115251.
Zeeshan, M., Haydar, S., Tabraiz, S., 2017. Effect of Fixed Media Surface Area on Biofouling and Nutrients Removal in Fixed Film Membrane Bioreactor Treating Sewage at Medium and High Fluxes. Water, Air, & Soil Pollution 228, 377.
Zhang, G., Zhang, F., Ding, G., Li, J., Guo, X., Zhu, J., Zhou, L., Cai, S., Liu, X., Luo, Y., 2012. Acyl homoserine lactone-based quorum sensing in a methanogenic archaeon. The ISME Journal 6, 1336.
Zhang, Y., Li, J., Liu, F., Yan, H., Li, J., Zhang, X., Jha, A.K., 2019. Specific quorum sensing signal molecules inducing the social behaviors of microbial populations in anaerobic digestion. Bioresource Technology 273, 185-195.
Zhou, J., Deng, Y., Shen, L., Wen, C., Yan, Q., Ning, D., Qin, Y., Xue, K., Wu, L., He, Z., 2016. Temperature mediates continental-scale diversity of microbes in forest soils. Nature Communications 7, 1-10.

## List of Figures

688 non-sterile fed AnMBR at 4 ℃; sAnMBR_15C: sterile fed AnMBR at 15 ℃; AnMBR_15C:
689 non-sterile fed AnMBR at 15 ℃. p value was obtained from t-test.

690 Figure 5 a) Non-metric multidimensional scaling (NMDS) plot of reactor communities. Each
691 point represents the community structure of the biofilm or sludge at 15 ℃ (rectangle) and
692 4 ℃ (circle); b) Relative abundance bar chart of all archaea (genus-level); c) Relative
693 abundance bar chart of 30 most abundant bacteria (genus-level). Minimum percentage
694 relative abundance of 1.0 was considered for the selection of abundant bacteria. An's' prefix
695 before the reactor code denotes sterile feed, _B denotes biofilm, _S denotes sludge, and 15C
696 and 4C are temperatures of 15℃ and 4℃. LCBD; local contribution of beta diversity, higher
697 LCBD means the sample has more unique species.

698 Figure 6 The 25 most abundant immigrant bacteria in reactors fed with non-sterile sewage; a)
699 immigrants in biofilms at 15 ℃; b) immigrants in biofilms at 4 ℃; c) immigrants in sludge at
700 15 ℃; d) immigrants in sludge at 4 ℃. Minimum percentage relative abundance of 0.01 was
701 considered for the selection of abundant immigrant bacteria. An's' prefix before the reactor
702 code denotes sterile feed, _B denotes biofilm, _S denotes sludge, and 15C and 4C are
703 temperatures of 15℃ and 4℃.

704 Figure 7 Co-occurrence network of sludge and biofilm communities of all reactors. The
705 nodes in the network are coloured by modularity at the genus level and AHL. The connection
706 stands for strong (Pearson's R > 0.7) and significant ($p < 0.05$) correlations. Nodes were only
707 labelled for immigrant in 4 ℃ only (black), immigrant in 15 ℃ only (sky blue), immigrant
708 appeared at both temperatures (green) and emigrant in both temperatures (blue), Acyl
709 homoserine lacton (red). AHL abbreviations are; C4: C4-HSL; C8: C8-HSL; C10: C10-HSL;
710 C12: C12-HSL; OC4: 3-oxo-C4-HSL; OC10: 3-oxo-C10-HSL; OC12: 3-oxo-C12-HSL.

711

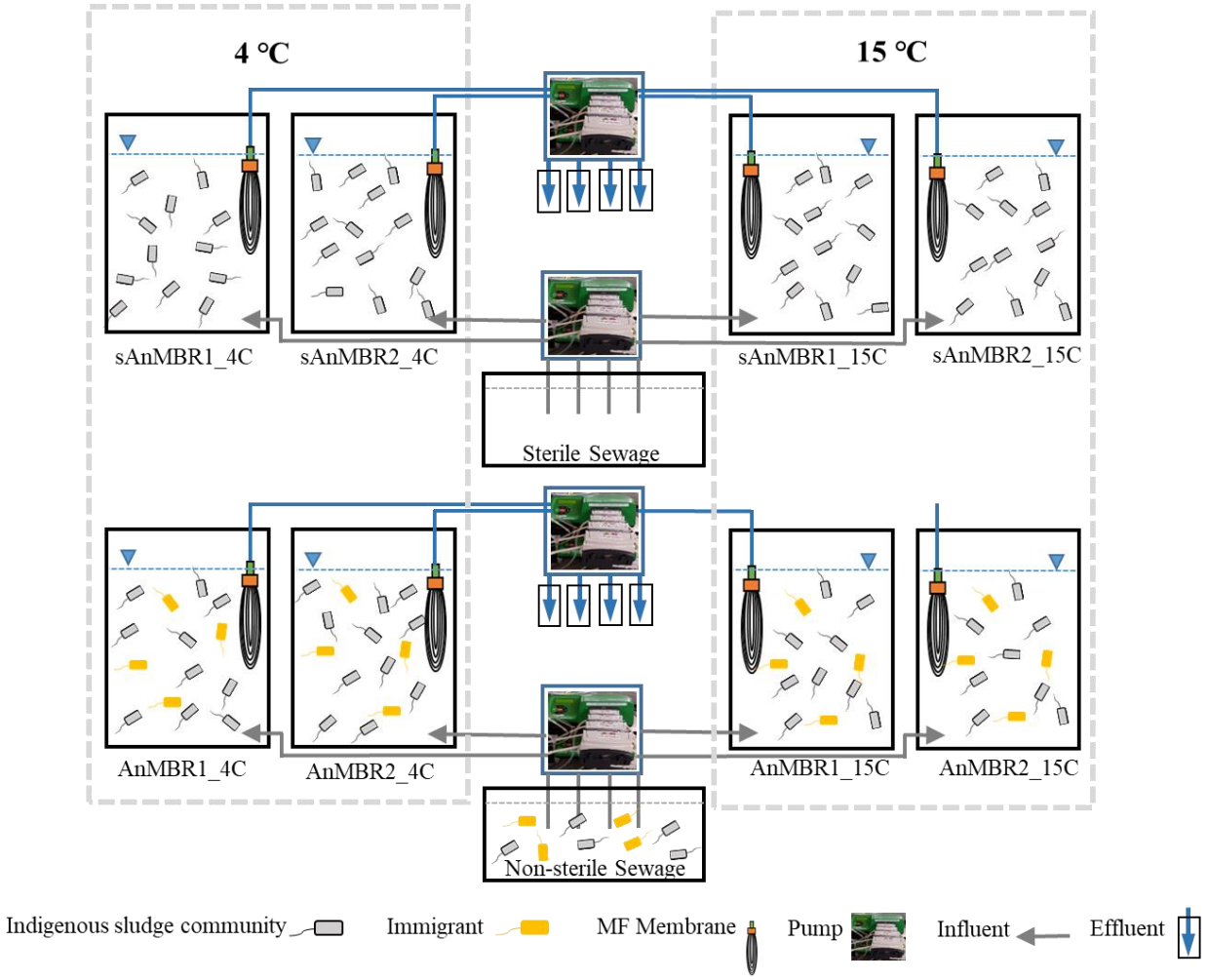


712

713 **Figure 1** Schematic diagram of experimental setup operated at 4 ℃ and 15 ℃ AnMBR_4C:
714 AnMBR at 4 °C fed with non-sterile sewage; sAnMBR_4C: AnMBR at 4 °C fed with sterile
715 sewage; AnMBR_15C: AnMBR at 15 °C fed with non-sterile sewage; sAnMBR_15C:
716 AnMBR at 15 °C fed with sterile sewage.

717

718

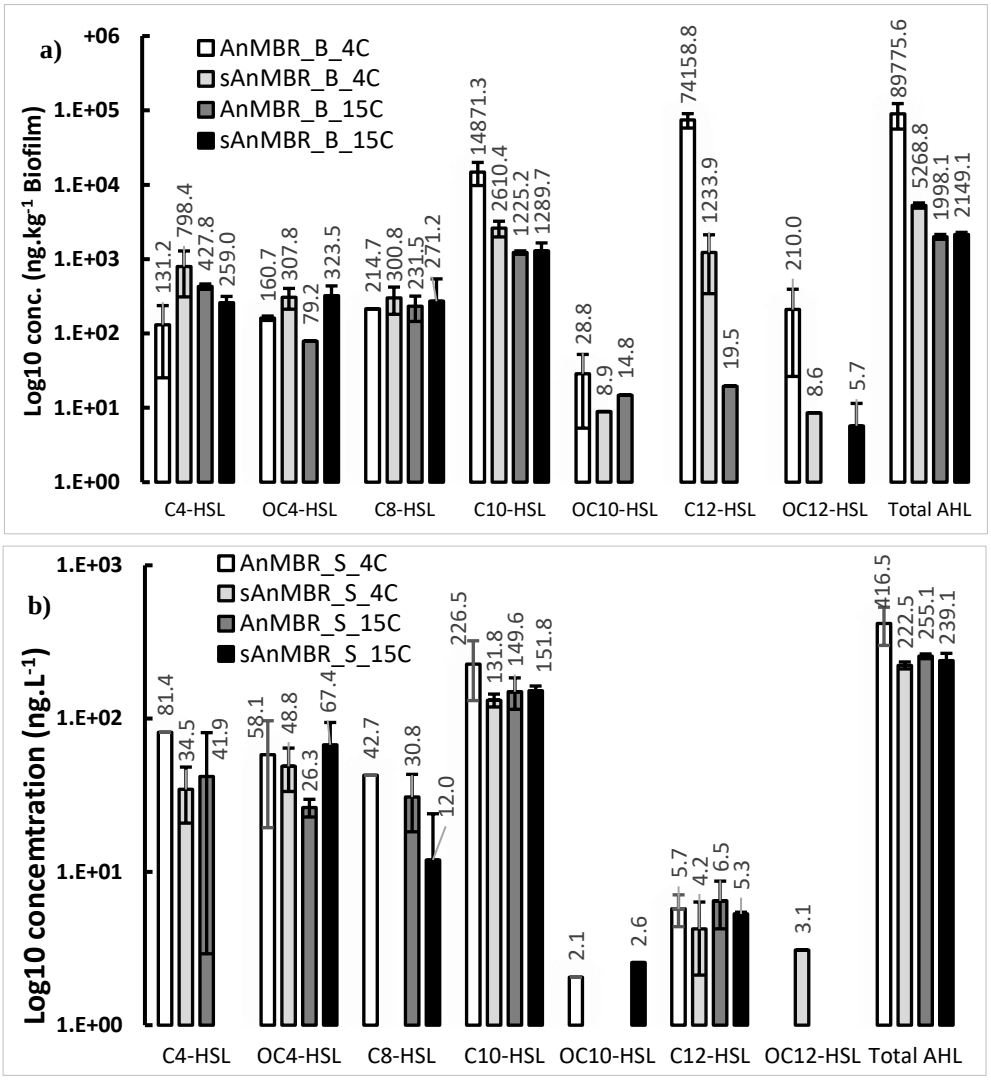


**Figure 2** AHL concentration in the (a) biofilms (wet biomass) and (b) sludge of AnMBR operated at 4 ℃ and 15 ℃ fed with UV-sterilised and non-sterilised sewage (error bars show standard deviation; n = 2); the y-axis has a logarithmic scale. AnMBR_BF_4C: Biofilm of reactor at 4 °C fed with non-sterile sewage; sAnMBR_BF_4C: Biofilm of reactor at 4 °C fed with sterile sewage; AnMBR_S_4C: sludge of reactor at 4 °C fed with non-sterile sewage; sAnMBR_S_4C: sludge of reactor at 4 °C fed with sterile sewage. AHL abbreviations are; C4: C4-HSL; C6: C6-HSL; C8: C8-HSL; C10: C10-HSL; C12: C12-HSL; OC4: 3-oxo-C4-HSL; OC6: 3-oxo-C6-HSL; OC8: 3-oxo-C8-HSL; OC10: 3-oxo-C10-HSL; OC12: 3-oxo-C12-HSL.

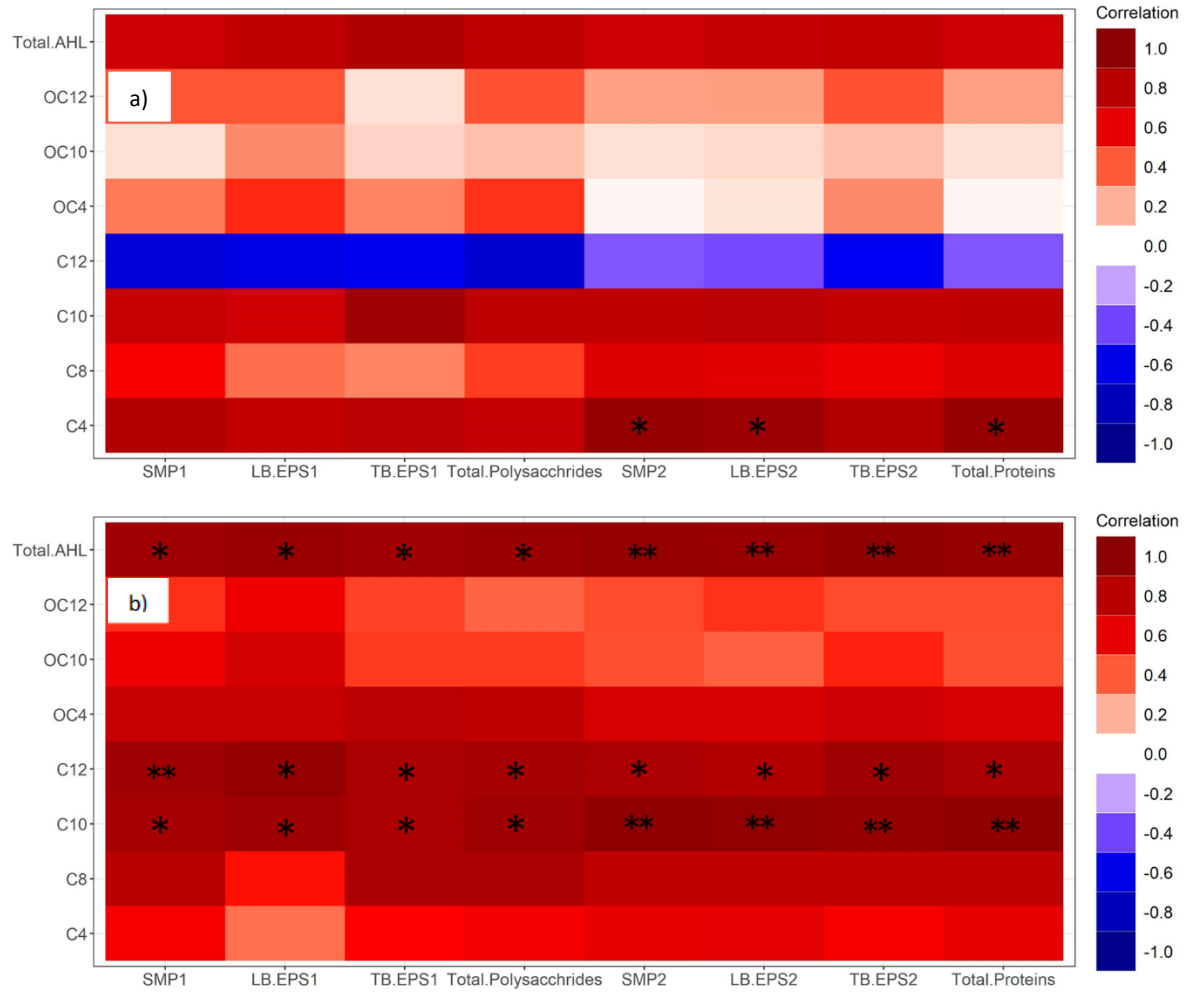


**Figure 3** Spearman correlation between proteins, polysaccharides and AHL present in biofilm and sludge of the AnMBR at 15 ℃ (a) and 4 ℃ (b). SMP1: polysaccharides in souble microbial product; LB.EPS1: polysaccharides in loosely bound extracellular polymeric substances; TB.EPS1: polysaccharides tightly bound extracellular polymeric substances; SMP2: proteins in souble microbial product; LB.EPS2: proteins in loosely bound extracellular polymeric substances; TB.EPS2: proteins in tightly bound extracellular polymeric substances, AHL abbreviations are; C4: C4-HSL; C6: C6-HSL; C8: C8-HSL; C10: C10-HSL; C12: C12-HSL; OC4: 3-oxo-C4-HSL; OC6: 3-oxo-C6-HSL; OC8: 3-oxo-C8-HSL; OC10: 3-oxo-C10-HSL; OC12: 3-oxo-C12-HSL. The asterisk (*) indicates $p < 0.05$ while double asterisk (**) indicates $p < 0.01$.

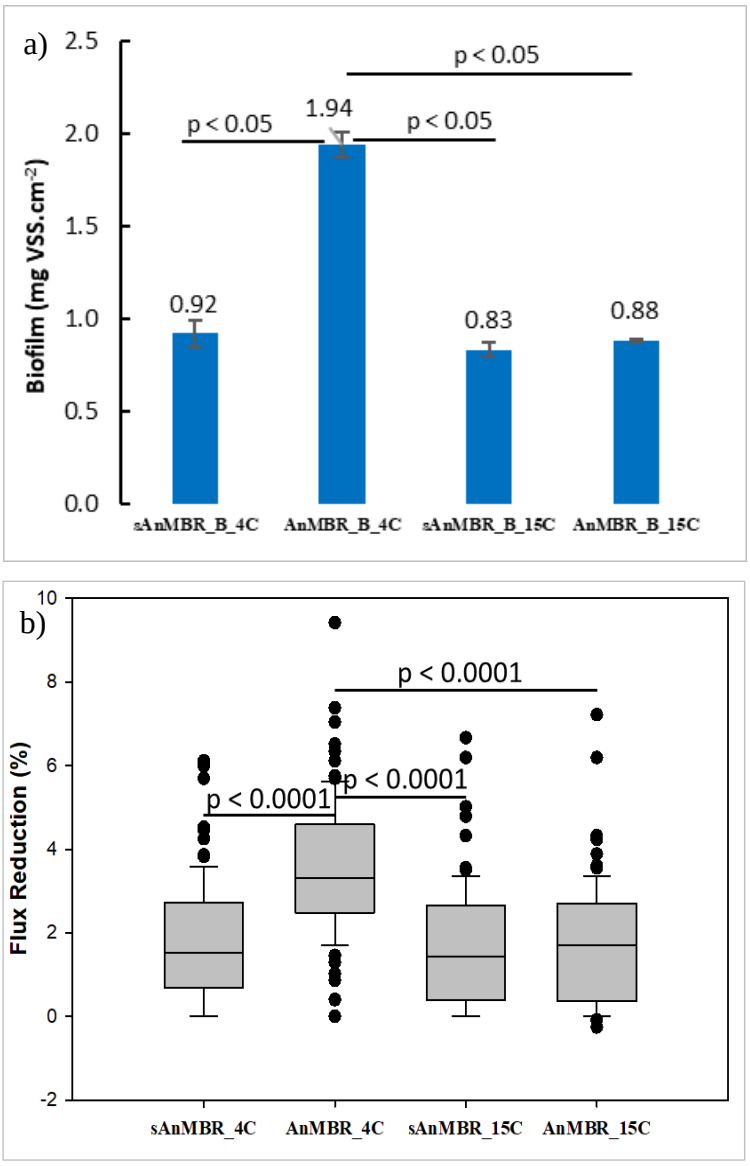


**Figure 4** a) Biomass on the biofilm per unit area, b) box plot of daily average flux reduction percentage of duplicates (110 days), sAnMBR_4C: sterile fed AnMBR at 4 ℃; AnMBR_4C: non-sterile fed AnMBR at 4 ℃; sAnMBR_15C: sterile fed AnMBR at 15 ℃; AnMBR_15C: non-sterile fed AnMBR at 15 ℃. *p* value was obtained from t-test.

784

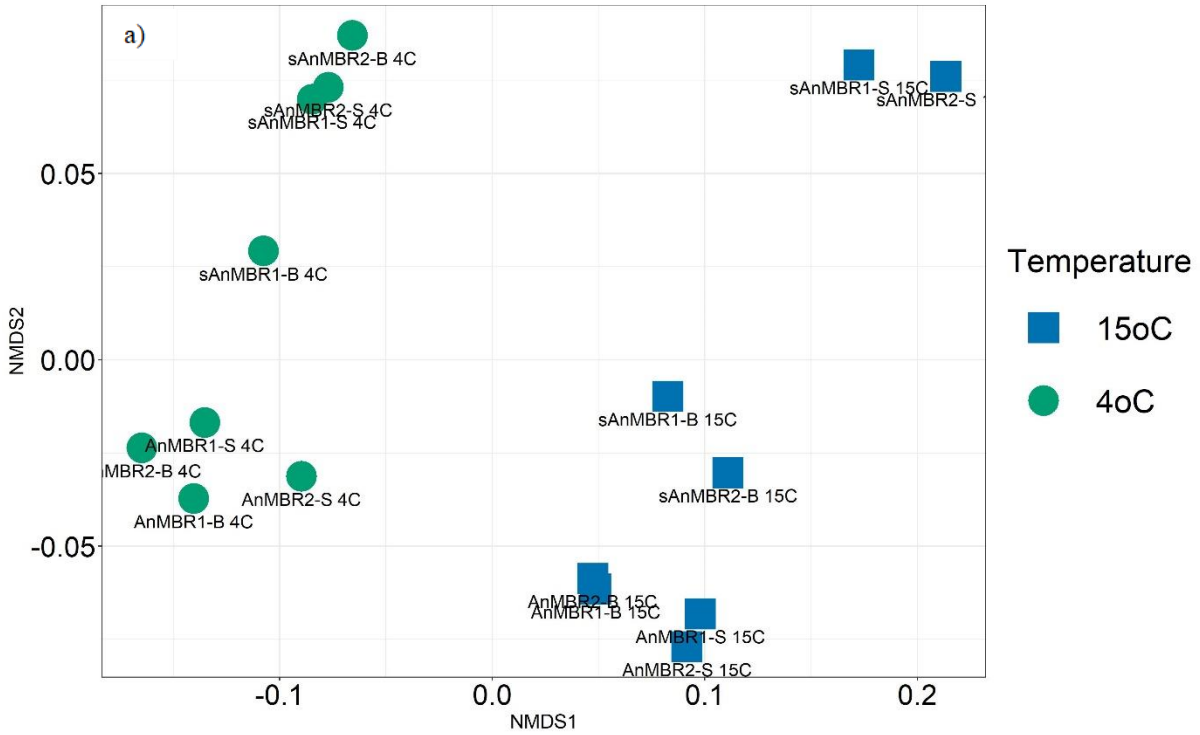


785

786

787

788

789

790

791

792

793

794

795

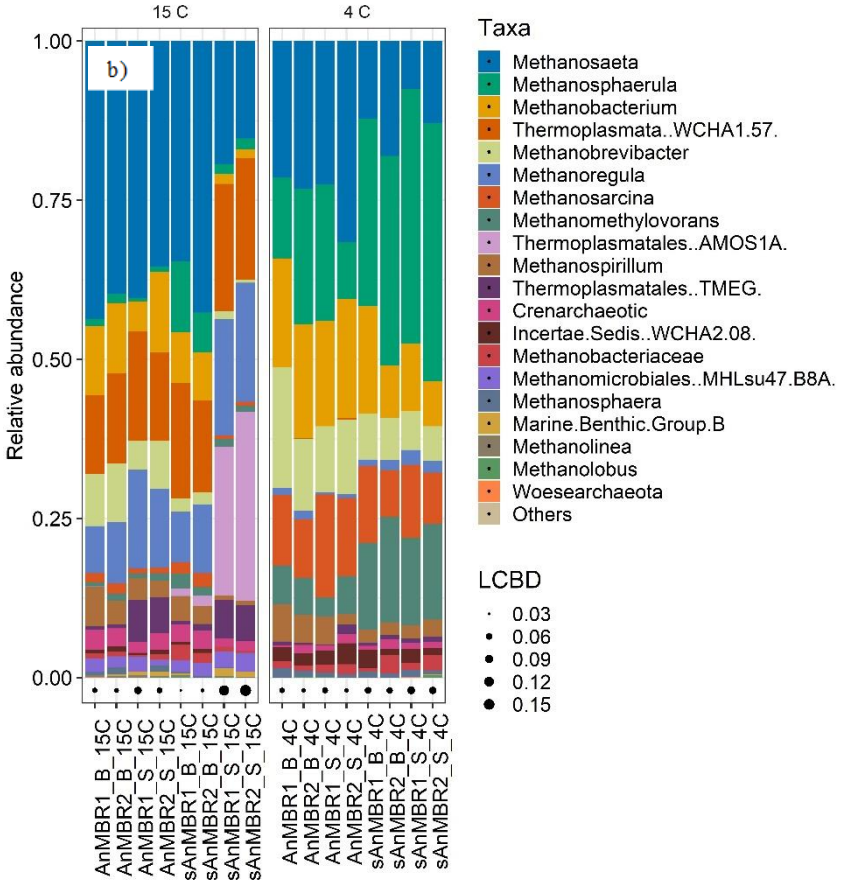

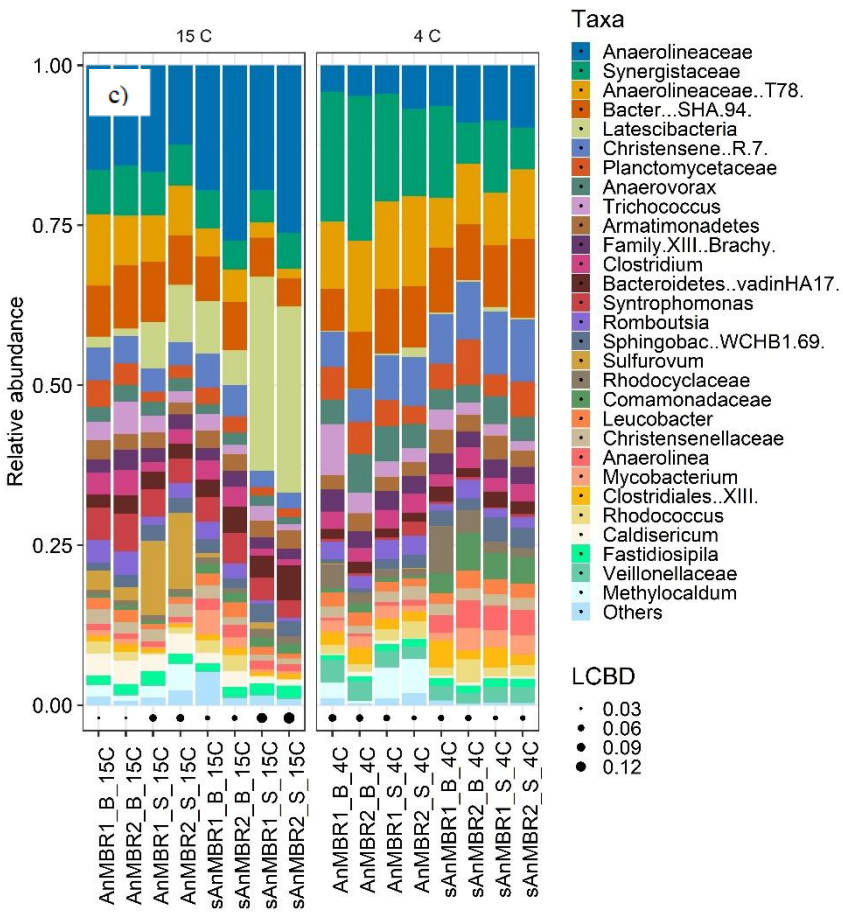


**Figure 5** a) Non-metric multidimensional scaling (NMDS) plot of reactor communities. Each point represents the community structure of the biofilm or sludge at 15 ℃ (rectangle) and 4 ℃ (circle); b) Relative abundance bar chart of all archaea (genus-level); c) Relative abundance bar chart of 30 most abundant bacteria (genus-level). Minimum percentage relative abundance of 1.0 was considered for the selection of abundant bacteria. An's' prefix before the reactor code denotes sterile feed, _B denotes biofilm, _S denotes sludge, and 15C and 4C are temperatures of 15℃ and 4℃. LCBD; local contribution of beta diversity, higher LCBD means the sample has more unique species.

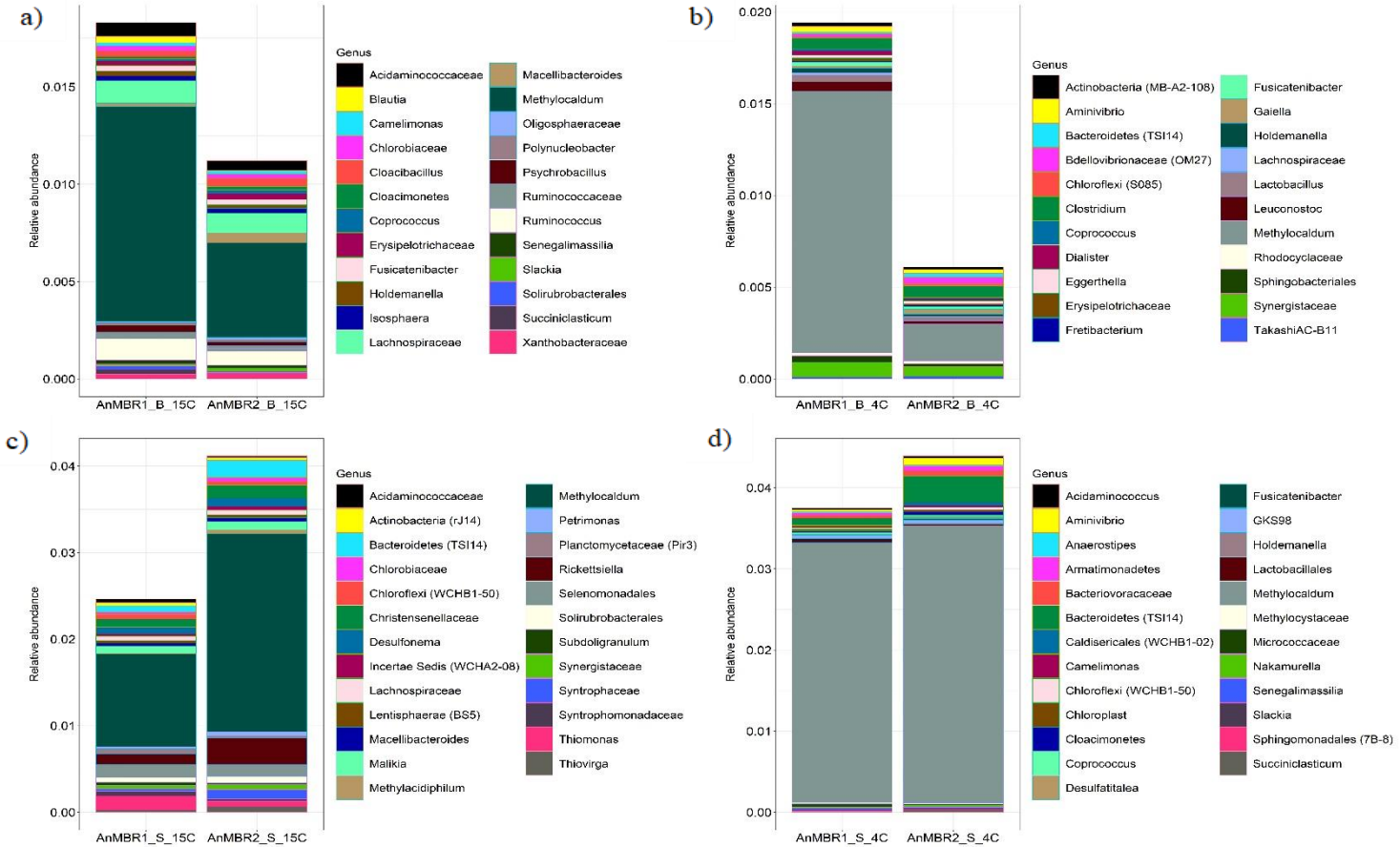


**Figure 6** The 25 most abundant immigrant bacteria in reactors fed with non-sterile sewage; a) immigrants in biofilms at 15 °C; b) immigrants in biofilms at 4 °C; c) immigrants in sludge at 15 °C; d) immigrants in sludge at 4 °C. Minimum percentage relative abundance of 0.01 was considered for the selection of abundant immigrant bacteria. An's' prefix before the reactor code denotes sterile feed, _B denotes biofilm, _S denotes sludge, and 15C and 4C are temperatures of 15°C and 4°C.

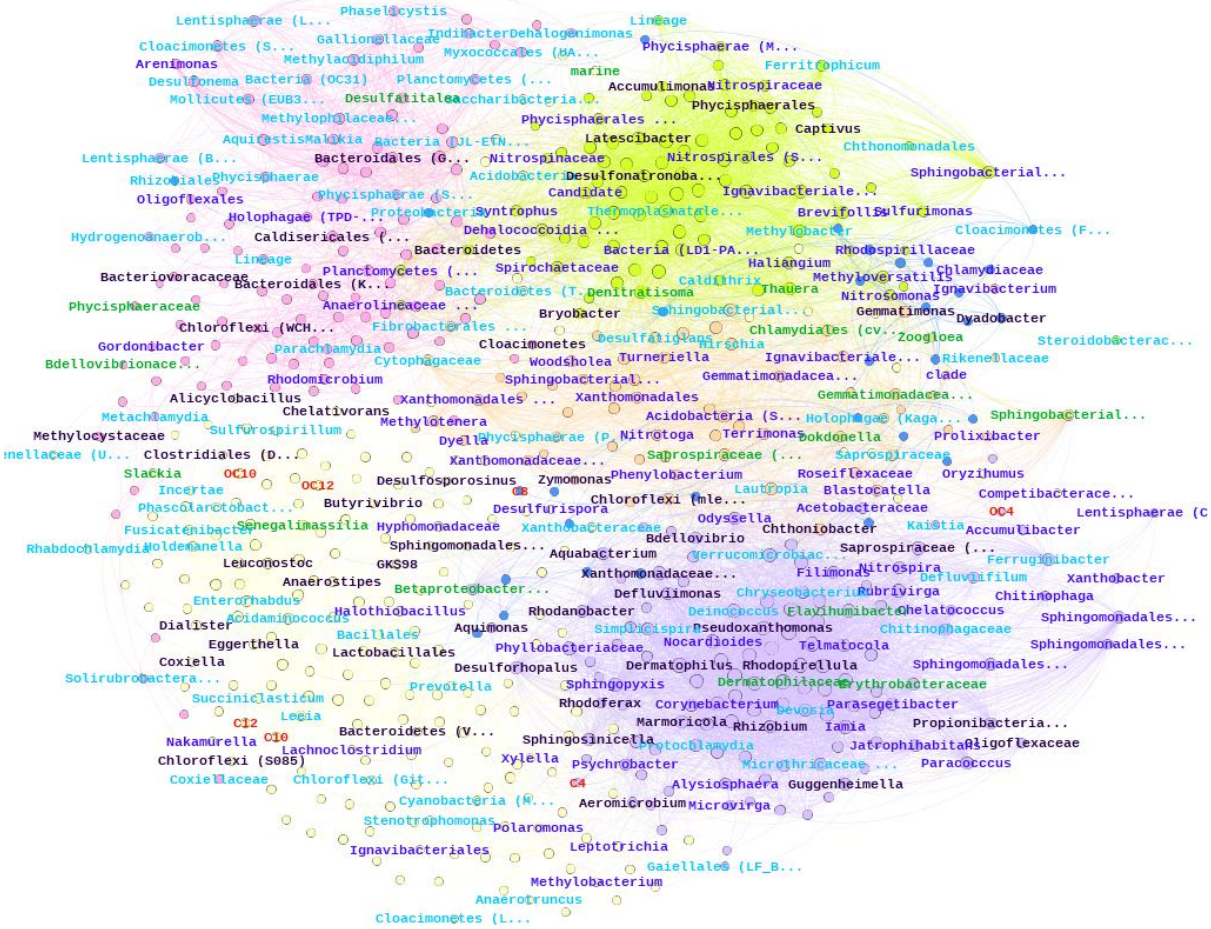


833

834 **Figure 7** Co-occurrence network of sludge and biofilm communities of all reactors. The
835 nodes in the network are coloured by modularity at the genus level and AHL. The connection
836 stands for strong (Pearson's R > 0.7) and significant ($p < 0.05$) correlations. Nodes were only
837 labelled for immigrant in 4 ℃ only (black), immigrant in 15 ℃ only (sky blue), immigrant
838 appeared at both temperatures (green) and emigrant in both temperatures (blue), Acyl
839 homoserine lacton (red). AHL abbreviations are; C4: C4-HSL; C8: C8-HSL; C10: C10-HSL;
840 C12: C12-HSL; OC4: 3-oxo-C4-HSL; OC10: 3-oxo-C10-HSL; OC12: 3-oxo-C12-HSL.

841